Comparison of wind and wind shear climatologies derived from high-resolution radiosondes and the ECMWF model

K. Houchi, A. Stoffelen, G.J. Marseille, J. de Kloe

Comparison of wind and wind shear climatologies derived from high-resolution radiosondes and the ECMWF model

K. Houchi,[1,2,3] A. Stoffelen,[1] G. J. Marseille,[1] and J. De Kloe[1]

Received 12 September 2009; revised 5 July 2010; accepted 13 July 2010; published 30 November 2010.

[1] The climatology of atmospheric horizontal wind and its vertical gradient, i.e., wind shear, is characterized as a function of climate region. For a better representation of the average atmospheric wind and shear and their variabilities, high-resolution radiosonde wind profiles up to about 30 km altitude are compared with the collocated operational ECMWF model for short-range forecast winds. Statistics of zonal and meridional winds are established from both data sets. The results show mainly similarity in the probability distributions of the modeled and observed horizontal winds, practically at all levels of the atmosphere, while at the same time the vertical shear of the wind is substantially underestimated in the model. The comparison of shear statistics of radiosonde and ECMWF model winds shows that the model wind shear mean and variability are on average a factor of 2.5 (zonal) and 3 (meridional) smaller than of radiosondes in the free troposphere, while in the stratosphere, the planetary boundary layer results are more variable. By applying vertical averaging to the radiosonde data, it is found that the effective vertical resolution of the ECMWF model is typically 1.7 km. Moreover, it is found for individually collocated radiosonde model wind and shear profiles that the model wind may lack in some cases variability larger than 5 m s^{-1} and 0.015 s^{-1}, respectively, due mainly to the effect of lacking vertical resolution, in particular near the jets. Besides the general importance of this study in highlighting the difference in the representation of the atmospheric wind shear by model and observations, it is more specifically relevant for the future Atmospheric Dynamics Mission (ADM-Aeolus) of the European Space Agency due for launch in 2012. The results presented here are used to generate a realistic global atmospheric database, which is necessary to conduct simulations of the Aeolus Doppler wind lidar in order optimize its vertical sampling and processing.

Citation: Houchi, K., A. Stoffelen, G. J. Marseille, and J. De Kloe (2010), Comparison of wind and wind shear climatologies derived from high-resolution radiosondes and the ECMWF model, *J. Geophys. Res.*, *115*, D22123, doi:10.1029/2009JD013196.

1. Introduction

[2] With the increase of interest in high-resolution modeling in numerical weather prediction (NWP) and climate research, a more detailed description of the atmosphere dynamics and optical properties is highly needed. Progress is possible because of the exponential development in high-performance computing and advances in instrumentation and measurement techniques, in particular at high resolution. Over the last decade, various and important projects exploiting high-resolution observations were accomplished, including SPARC (Stratospheric Processes and Their Role in Climate), FASTEX (Fronts and Atlantic Storm Track Experiment), etc. These are motivated by the necessity of understanding and resolving many atmospheric processes occurring generally at mesoscale and smaller scale and which most current weather models fail to resolve, such as convection, cloud development, gravity waves, turbulence, etc. These effects are generally parameterized using the local mean wind and vertical wind shear as input, among other things. Recall that, in this manuscript, the vertical gradient of the horizontal wind is referred to as vertical wind shear. For a definition, see section 2.4. To develop these parameterization schemes, detailed knowledge of the spatial scales of the dynamical processes represented in NWP or climate models is indispensable. The determination of the mean state and variability of the atmosphere can be based on measurements or on models. *Håkansson* [2001] described global wind statistics utilizing 31 ECMWF (European Centre for Medium-Range Weather Forecasts) model levels of analysis fields and low-resolution radiosonde observations, reported only at standard and significant levels [*Office of the Federal Coordinator for Meteorology* (*OFCM*), 2006]. He shows that, except near the surface, there is a

[1]Weather Department, Royal Netherlands Meteorological Institute, De Bilt, Netherlands.
[2]Department of Applied Physics, Eindhoven University of Technology, Eindhoven, Netherlands.
[3]Laboratoire de Météorologie Dynamique, École Polytechnique, Palaiseau, France.

0148-0227/10/2009JD013196

large similarity in the wind and shear statistics for both collocated data sets, despite the limited vertical representation in the ECMWF model. One may conclude that the representation of the atmospheric wind by standard and significant radiosonde levels and the ECMWF model is similarly poor. The aim of this study is to statistically describe the climatological wind and wind shear characteristics of the first 30 km above the Earth surface at higher vertical detail. This is done by collocating high-resolution radiosonde observations with the ECMWF Short Range Forecast (SRF) model, such that the results may be compared to *Håkansson* [2001]. The effect of vertical smoothing in the radiosonde on both wind and shear variabilities is investigated, first on individual collocated radiosondes-ECMWF profiles and then statistically.

[3] The ECMWF model (see section 2.1 for the model description) offers a good quality atmospheric wind with a global coverage and with relatively high resolution. On the other hand, radiosonde balloons are currently the only observing system providing continuous vertical wind profiles at very high resolution from the surface to high altitudes (including a large part of the stratosphere), although limited to mainly the Northern Hemisphere continents. The typical balloon ascent rate is about 5 m s^{-1} [*Brock and Richardson*, 2001], with only 10%–15% variation in ascent speed along the trajectory, although in the presence of gravity waves, the variation may be occasionally higher [*Shutts et al.*, 1988; *Kitchen and Shutts*, 1990; *Shutts et al.*, 1994], as well as in strong convection.

[4] An overview and a detailed description of both the model and radiosonde observations are given in section 2. However, 3-D wind profile observations are one of the most important and lacking meteorological quantities in the current global observing system (GOS) [*World Meteorological Organization* (*WMO*), 2008]. Deficiencies, notably in the temporal and spatial coverage of wind observations in the current GOS, are hampering the rapid progress in operational weather forecasting and climate-related studies. The future mission of the European Space Agency (ESA), AEOLUS Atmospheric Dynamics Mission (ADM), which in fact motivated this study, will provide more homogeneous global wind profile coverage. This mission, due for launch in 2012, aims to retrieve global wind profiles of the lowermost 30 km of the atmosphere using a Doppler wind lidar (DWL) operating in the ultraviolet (at 355 nm) part of the electromagnetic spectrum [*Stoffelen et al.*, 2005]. Several studies demonstrated [*Stoffelen et al.*, 2006; *Zagar et al.*, 2008; *Tan et al.*, 2007; *Marseille et al.*, 2008a, 2008b, 2008c], using different techniques, that Aeolus measurements would have a significant impact on NWP and climate models. In addition, further understanding of atmospheric dynamics and climate processes is also expected from this mission (see ESA's Web site: http://www.esa.int/esaLP/ESAEPG2VMOC_LPadmaeolus_0.html).

[5] ADM-Aeolus vertical range bin resolution is limited by 24 bins spread over 30 km height. The distribution of these vertical bins is being optimized by conducting simulations of Aeolus-DWL vertical sampling in realistic global atmospheric conditions, i.e., by considering the complex optical and dynamical heterogeneities of the atmosphere. Since the ECMWF model fields are continuous in space and (almost) in time, they may be combined with any high-resolution optical data set, such as the Cloud-Aerosol Lidar and Infrared Pathfinder Satellite Observations (CALIPSO). On the other hand, collocations between, e.g., CALIPSO and high-resolution radiosonde data are rare. However, to use ECMWF collocations for ADM simulation, we need to investigate what wind scales are represented by the ECMWF model. By characterizing the wind and wind shear climatology from the ECMWF model and high-resolution radiosonde observations, one may develop an ability to build a realistic global atmospheric database needed for Aeolus-DWL simulations.

[6] To this end, available worldwide high-resolution radiosonde observations were collected. A specific year, 2006, with the most abundant SPARC high-resolution radiosonde data has been collocated with short-range forecasts of the ECMWF model (ECMWF-SRF), as described in section 2. This section also includes the available global data coverage and the definition of the climate regions as used here. This is followed by a discussion about the presence of outliers in radiosonde wind measurements and the difference in accuracy of the various wind-finding systems used to collect the data: radiotheodolite, LORAN, and GPS. In section 3, an example of collocated radiosonde-ECMWF wind and shear profiles is shown and discussed. It is followed by the statistics of zonal and meridional wind profiles and the resulting shear for different climate regions. The radiosonde horizontal drift from its launch position was also characterized for the different climate regions in order to verify the validity and consistency of the comparison between the ECMWF model and radiosonde climatologies, since we simplified the spatial collocation to the radiosonde ground location, i.e., not following the radiosonde ascent trajectory. In addition, to verify the consistency of the 2006 SPARC collocated statistics, we established similar statistics from new generation and more accurate radiosoundings (BADC, AMMA, and De Bilt; described in section 2) and by processing 9 years of SPARC data in addition to 2006. The effect of vertical smoothing (resolution) on wind and wind shear variability is investigated, first on individual collocated profiles and then on the statistics of wind and shear. Finally, by comparing the wind shear statistics obtained from the ECMWF model and the radiosonde observations at different resolutions, we could determine the effective vertical resolution of the ECMWF model. In the concluding section, the major results are summarized.

2. Data and Method

2.1. Data and Collocation

2.1.1. ECMWF Model Versus High-Resolution Radiosondes: Overview

[7] The ECMWF model provides a good quality and global atmospheric wind at relatively high resolution. It is important to recall that on 2 February 2006 the ECMWF model moved from 60 to 91 (p_L60 to p_L91) vertical levels, reaching an altitude of about 80 km in both versions. Figure 1 shows an enhancement in the number of levels for the L91 model version, particularly in the first 15 km. The L60 model has a horizontal spectral truncation of T511 [*Riddaway*, 2001], which corresponds to a horizontal mesh size of 40 km, while for the L91 model it is T799 (~25 km). But the effective horizontal resolution is larger as shown by

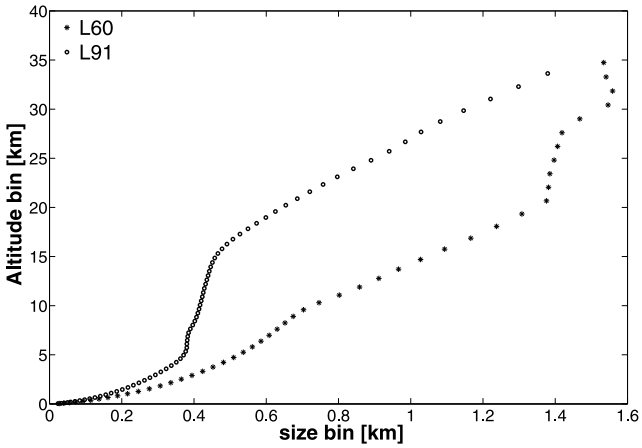

Figure 1. Increasing vertical separation of ECMWF model levels with altitude for the two model versions, L60 (blue) and L91 (red). Both models have irregular size bins between one level and another. Notice that the number of levels is enhanced particularly in the PBL and free troposphere for the L91 model.

Stoffelen et al. [2008]. The ECMWF horizontal wind power spectra drop substantially for a wavelength below about 250 km, thus denoting the effective horizontal resolution of the model. In line with this, *Skamarock* [2004] showed for different grid sizes (22, 10, and 4 km configurations of the Weather Research and Forecast (WRF) model) that the effective horizontal resolution is generally around 7 times the grid resolution. Additional new parameterizations and their effect on the atmospheric variability of the ECMWF model are reported by *Bechtold et al.* [2008]. But tests with collocated De Bilt radiosoundings and the ECMWF model, over the year 2008, did not show substantial changes of the results as reported in this manuscript (see Figure 7c).

[8] On the other hand, radiosonde balloons are the only observing system that provides vertical wind profiles at very high resolution (up to 1 s) from the surface to high altitudes, continuously and covering a large part of the stratosphere. However, they are limited mainly to the Northern Hemisphere continents and with very sparse coverage over ocean, tropical, and Southern Hemisphere areas. In addition, these radiosoundings were for a long time devoted only to weather forecasting; therefore, they were archived only at standard and significant levels, which are required to be sent to operational weather centers via the global telecommunication system (GTS) for real-time use [*Hamilton and Vincent*, 1995]. Worldwide, there are more than 1500 stations with varying temporal coverage records [*Durre et al.*, 2006]. In the early days, not all radiosonde data contained wind measurements, and wind quality is being improved progressively following advances in the wind-finding systems, starting from optical radiotheodolite to LORAN (long range navigation), and the new generation of modern GPS (global positioning system) systems. For reference, a useful description of radiosonde instruments and data interpretation, including history, development, and future prospects, may be found in the two articles of *Brettle and Galvin* [2003] and *Galvin* [2003].

2.1.2. Data Coverage and Collocation Procedure

[9] Here 92 stations with high-resolution (6 s) radiosonde data over the 10 year period from 1998 to 2007 (available through the SPARC project Web site ftp://atmos.sparc.sunysb.edu/pub/sparc/hres) were fully exploited in this study. The most continuous in time of the 2006 radiosonde data from the British Atmospheric Data Centre (BADC) [see *UK Met Office*, 2009], the African Multidisciplinary Monsoon Analysis (AMMA), and the "De Bilt" radiosondes at Royal Netherlands Meteorological Institute (KNMI, Netherlands) are further selected for the analysis. We briefly note that SPARC observations are intended for the study of gravity waves [*Allen and Vincent*, 1995] and AMMA for the African monsoon, while BADC and De Bilt are raw data of standard resolution radiosondes dedicated for weather forecasting. These data cover a large part of the Northern Hemisphere with highest density in the United States; however, only two stations are available in the Southern Hemisphere (Falkland Islands and Saint Helena). It is important to mention that we noticed a difference in the accuracy between SPARC and the rest of the data sets due to the difference in the wind-finding system used to collect each data set. BADC, AMMA, and De Bilt data sets, based on combined LORAN and GPS system, have a better accuracy of wind and ascent height measurements than the SPARC radiotheodolite-based data. Therefore, they are analyzed separately from SPARC to avoid misinterpretation of the statistics. The focus was in particular on the ascent height increment (dz) of the SPARC radiosondes, which has uncertainty that degrades the computation of wind shear, du/dz. The 2006 SPARC radiosondes, totaling 85 stations for both 12 UTC and 00 UTC, are collocated with ECMWF Short Range Forecast (ECMWF-SRF) fields for a first comparison between model and observations. The spatial collocation is performed according to the radiosonde launch ground location, i.e., model wind fields at the different model levels are extracted from the ECMWF archive and interpolated to the ground location (latitude, longitude) of the radiosonde launch (not following the radiosonde trajectory). The temporal collocation is done with the 12 h SRF, i.e., a radiosonde launched for instance at 12 UTC (00 UTC) is thus compared with a SRF initiated at 00 UTC the same day (12 UTC the day before). The main reason for using the forecast model rather than analyses is to avoid what is called a generally "incestuous" comparison between model and observations, since the analyses model fields may already contain the comparison radiosonde observations. Also, the difference in the number of levels between the p_L60 and p_L91 model versions is taken into account during the analysis by interpolating both to 60 m vertical resolution. However, since we focus only on the first 30 km of the atmospheric winds, which generally also correspond to the maximum altitude reached by the radiosonde balloons, only 76 vertical model levels are used, which cover this part of the atmosphere.

[10] Before performing the analysis, both ECMWF model and radiosonde data sets were distributed over seven climate zones, which we define as follows: Northern Hemisphere/Southern Hemisphere polar (70°–90°), Northern Hemisphere/Southern Hemisphere midlatitude (40°–70°), Northern Hemisphere/Southern Hemisphere subtropics (20°–40°), and tropics (20°S–20°N). The global coverage of the available and analyzed data sets, including their distribution over the defined climate regions, is shown in the map of Figure 2. This is also summarized in Table 1. We note that the BADC and AMMA have a time resolution of 2 s, while it is 10 s for De

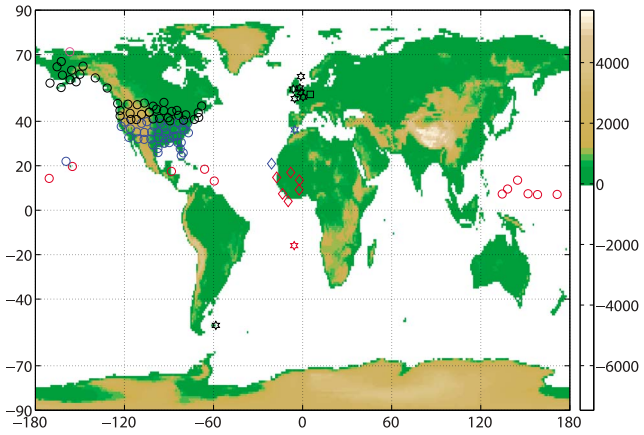

Figure 2. The geographical locations of analyzed high-resolution radiosonde data sets: SPARC (circles), BADC (hexagrams), AMMA (diamonds), and De Bilt (Square) as function of climate regions, successively for the tropics (red), subtropics (blue), midlatitudes (black), and polar (magenta). Note the orography (brown) in the map which may explain the appearance of lee waves for some stations, in particular in the Rocky Mountains. The right legend bar from zero meter and up indicates the altitude of the Earth surface from sea level; below sea level is masked white here.

Bilt. Radiosondes with time resolutions of 2, 6, and 10 s correspond successively to vertical height increments (dz) of about 10, 30, and 50 m. We report the results at the same resolution when needed, mainly at about 60 m resolution for comparison with SPARC. We sometimes omit deliberately to mention 12 UTC or 00 UTC, since we found similar results at both UTC times for each subdata set. This is due to the fact that the stations extend over a large longitudinal band covering thus a large range of time zones of more than 6 h. So the data cover particular UTC local time zone (day time and nighttime) launches. For instance, for the midlatitudes and time containing mixed subtropical stations at 12 UTC (00 UTC), the data cover a time zone extending from at least 3 AM to 9 AM (3 PM–9 PM).

2.2. Quality Control and Wind-Finding System Characteristics

[11] Before establishing the statistics of wind and wind shear, two major issues are faced. The first issue is related to the amount of unrealistic wind observations present in the raw SPARC high-resolution data, even though a strong quality control was applied [*National Climate Data Center* (*NCDC*), 1998] at the University Corporation for Atmospheric Research and Joint Office of Science Support (UCAR/JOSS). The second issue is related to the limited accuracy of the ascent height intervals or what we call shear intervals (dz), compromising the wind shear computation. Both issues are related to the radiotheodolite wind-finding system used to collect these SPARC data and which is generally less accurate than the LORAN and GPS systems. To deal with this issue, a statistical quality control (QC) method was developed. The method (see section 2.3) cleans the SPARC data from unrealistic (outlier) atmospheric wind and wind shear observations, including unrealistic shear intervals (dz). More details on the overall issues in this subsection may be found in the work of *Stoffelen et al.* [2009].

2.3. Removal of Outliers

[12] The statistical quality control consists first of accumulating the raw information of wind, wind shear, and shear intervals (dz) into probability density functions (PDFs) of these variables at different levels of the atmosphere with uniform vertical bins of 1 km interval. Percentiles of these PDFs are subsequently computed with very fine percentiles sampling at the tails, i.e., the percentile ranks are very closely separated. For such small change in the percentile, e.g., 0.1%, at the tails of the PDF, the change in the observed quantities (wind, wind shear, and dz) is expected to be very small and regular. However, outliers fall generally far away from the common PDF, implying they are implausible realizations of the natural wind, shear, and dz distributions and thus cause a relatively big jump in the location of subsequent percentiles at the extremities of the PDFs, particularly notable in case of very dense percentile sampling. By eliminating such large jumps, the maximum number of data points removed at each 1 km vertical bin does not exceed 1/1000 on either PDF tail. In fact, this amount is only reached when the number of data available in a vertical bin is small, as for the NH polar region where we only have one station. For the other regions, most outlier percentages fall below the 0.1% and above the 99.9% percentile profiles. Therefore, only 1/1000 data points on both sides of the tails are generally removed. The statistical quality control was carefully tested and visually checked. And we made sure that the wind values used are not exceeding the tolerance limits of the extreme values [*DiMego et al.*, 1985], as required by WMO. A manuscript describing the method in more detail is under preparation.

2.4. Analysis Method and Definitions

[13] After quality control of wind, wind shear, and shear interval (dz) of the radiosonde data, the subsequent processing step consists, as for the QC, of accumulating wind and shear information (including the drift of the radiosonde)

Table 1. Distribution of Radiosoundings Over the Defined Climate Regions for Stations of SPARC, BADC, AMMA, and De Bilt Over the Years as Indicated

Periods/Stations	Total	Tropics	Subtropics	Midlatitudes	Polar
SPARC 2006	85	9	37	38	1
1998–2007	85 + 7[a]				
BADC 2006	9	1 (SH: Saint Helena)	1 (Gibraltar)	7 (1 SH: Falklands Islands)	-
AMMA 2006	6	5	1 (Nouadhibou)	-	-
De Bilt 2006	1	-	-	1	-

[a]Seven stations among a total of 92 are distributed unequally over climate regions from 1 year to another. We note here that only two stations from the Southern Hemisphere midlatitudes (Falkland Islands and Saint Helena) are available from the BADC data.

at different levels of the atmosphere with uniform vertical bins of 1 km intervals. This is done for both observations and model. To establish the observation statistics, we used mainly 12 s (~60 m) averages rather than 6 s (raw) data in order to reduce the random noise, in particular for the shear interval (dz). Recall that the quoted spatial resolution between parentheses is given as a rough indication, considering that the mean ascent rate of the radiosonde balloon is about 5 m s^{-1}, which is generally the case [*Brock and Richardson*, 2001]. The model profiles are interpolated to each 60 m vertical level before performing the statistics. The means and percentiles (successively: 10%, 25%, 50%, 75%, 90%) of each quantity are computed at each vertical atmospheric bin. The values obtained at each bin constitute thus the mean and percentile profiles, as can be seen in the overall results in section 3. The wind shear and the balloon drift profiles analyzed here are derived from wind profiles as follows: The wind shear vector $\boldsymbol{s}$ is defined as the variation of the horizontal wind vector $\mathbf{v} = (u, v)$ with height z (equation (1)),

$$\mathbf{s}_i = \frac{\mathbf{v}_{i+1} - \mathbf{v}_i}{z_{i+1} - z_i}, \tag{1}$$

with i indicating the level number $i = 1, N - 1$, and N, the total number of vertical levels, which depends on the vertical resolution used. u and v are the zonal and meridional winds. Notice that absolute values are considered for wind shear statistics in the next sections and plotted in decadic logarithmic scales (along the horizontal axis) as a function of shear height $(z_i + z_{i+1})/2$.

[14] We mention here that, in view of the limited accuracy of $dz = z_{i+1} - z_i$ for SPARC data, the mean of dz at each vertical bin is used to compute vertical changes in the horizontal wind as a proxy for the shear. So here $z_{i+1} - z_i$ (or dz) in equation (1) is not the dz reported by the individual radiosonde but the mean dz estimated at each vertical bin for each subdata set analyzed. However, $\mathbf{v}_{i+1} - \mathbf{v}_i$ reported by the individual radiosonde is taken as the zonal/meridional wind variation over dz. This approach of considering the climatological mean of dz inside the bin to compute the shear has been tested with more accurate GPS radiosonde data; i.e., Shear values obtained by this approach were compared with the nominal GPS radiosondes shear values and have showed very similar wind shear results (not shown).

[15] The radiosonde balloon drift at height level z_i is computed from the successively reported horizontal positions of the balloon with altitude. This is done by accumulating successive horizontal distances traveled by the balloon as given by equation (2),

$$\mathrm{Drift}(z_i)\sqrt{\left(\sum_{j=1}^{j=i} \mathrm{d}x_j\right)^2 + \left(\sum_{j=1}^{j=i} \mathrm{d}y_j\right)^2}, \tag{2}$$

where $\mathrm{d}x_j = 0.5(u_j + u_{j+1})\mathrm{d}t$ and $\mathrm{d}y_j = 0.5(v_j + v_{j+1})\mathrm{d}t$ are the zonal and meridional distances traveled by the radiosonde balloon from one atmospheric layer level j to another $j + 1$. z_i is the level height, where i indicates the level number at which the drift is computed.

[16] Because of the two limitations mentioned above in section 2.2 for SPARC data and to render the statistical interpretation easier, the radiosonde data from BADC, AMMA, and De Bilt (KNMI) based on more recent and accurate wind-finding systems (combined LORAN and GPS) are analyzed separately. The most useful and regular data over 2006 are selected for analysis. This is done by following the same procedure as for SPARC data, i.e., these data were subjected to the same QC, then distributed and segregated according to their location over the defined climate zones. The statistics from the different data sets, based on different wind-finding systems, have been compared, including the results of the Q-controlled wind, wind shear, and shear intervals. Furthermore, to check the validity and the consistency of the statistics obtained over 2006, the remaining 9 years of SPARC data for the period 1998 to 2007 were processed.

3. Results and Discussion

3.1. Collocated Radiosondes and Model Wind and Shear Profiles

[17] Figure 3 shows an example of individual wind and wind shear profiles of a high-resolution radiosonde at 6 s (~30 m) collocated with an independent ECMWF short-range forecast at 90.1°W 32.3°N on 30 December 2006 at 00 UTC. The ECMWF profiles broadly compare well in shape to the radiosonde profile but with clear differences between the profiles in both wind and shear, particularly in the detailed vertical structure. Substantial increases of wind shear are remarkable over up to 1 km extended depths in the lower troposphere, at tropopause height (8–15 km), and in the lower stratosphere. Figure 3 illustrates the more general observation in our data set that the vertical gradient of the horizontal wind is large for a typical high-resolution radiosonde ascent as compared to the ECMWF model. The ECMWF wind and shear profiles are very smooth, ignoring thus important vertical structures. The ECMWF model profile shown here is from the L91 model version.

3.2. Zonal/Meridional Wind and Shear Climate Statistics

[18] To investigate the atmospheric wind dynamics and its vertical gradient (shear), the analysis method described in section 2.4 is applied. The statistics for the horizontal wind and wind shear from collocated ECMWF model and high-resolution radiosonde observations have been established for a 1 year data set (2006). This was performed successively for zonal and meridional winds and over the defined climate regions. The results are presented here as percentile and mean profiles. The statistics of radiosonde balloon drifts are also provided. This is important to verify how valid the comparison between the model and observation climates is, since the collocation of the model wind is done only at the ground location of the radiosonde observations, i.e., not following the balloon trajectory ascent. Note that over short distances, i.e., less than 100 km, the climate is not expected to change much, so exact collocation appears less relevant for the comparison of climate data sets of radiosondes and ECMWF model. The results of the radiosonde balloon drift are first summarized for the different climate regions with the mean profiles, and then only the subtropical case is shown with mean and percentile profiles.

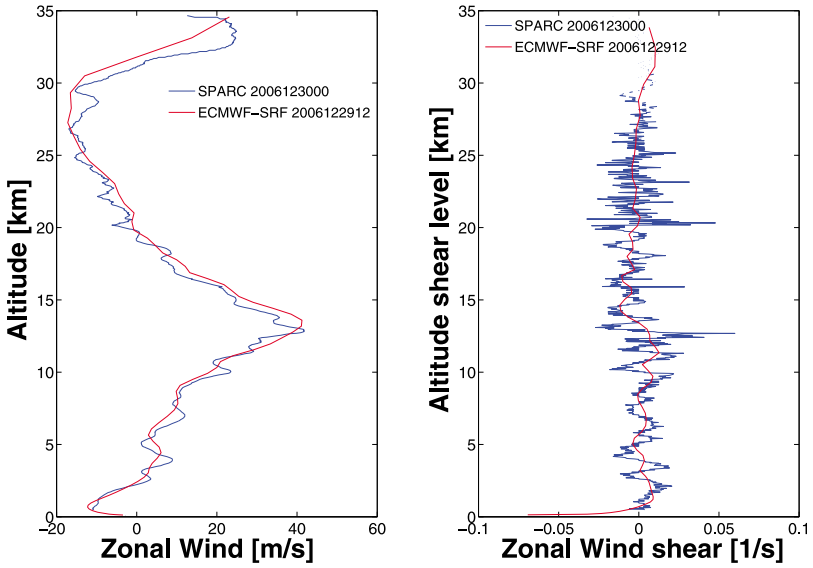

Figure 3. (left) Zonal wind and (right) wind shear collocation of the high-resolution radiosonde at 90.1°W–32.3°N from the SPARC data set (blue) with the ECMWF 12 h forecast (red). The time resolution of the radiosonde here is 6 s (~30 m). 2006122912 means that the 12 h forecast was initiated at 12 UTC on 29 December 2006, and verification time is 00 UTC on 30 December 2006.

3.2.1. Zonal Wind and Wind Shear

[19] Figure 4 shows the wind and wind shear statistics (means and percentiles) for high-resolution radiosondes and their corresponding model counterpart. Notice that the absolute wind shear values are plotted in decadic logarithm scale. The radiosonde and model wind statistics show a clear resemblance, while the wind shear statistics are different. This is observed in all climate regions (tropics, subtopics, midlatitudes, and polar). The difference in the shear statistics is due in particular to the limited effective vertical resolution of the ECMWF model, which does not capture the mesoscale and small-scale dynamical structures of the atmosphere. As mentioned in section 2.1, the ECMWF horizontal wind power spectra drop substantially for a wavelength below 250 km, leaving thus most atmospheric processes occurring below this scale (e.g., turbulence and convection) unresolved. However, *Håkansson* [2001] found similarity in wind and shear statistics between the ECMWF model and low-resolution radiosonde observations despite the limited vertical representation in the ECMWF model of 31 levels, except near the surface. This indicates that the low-resolution radiosondes lack substantial wind shear in the vertical, similar to the ECMWF model. Near the surface, the large wind shear found in the ECMWF model by *Håkansson* [2001], exceeding values of 0.1 (s^{-1}), is attributed to the misrepresentation of the pressure gradients at the lowest model levels (in turn arising from the misrepresentation of the topography). This includes the (erroneous) horizontal interpolation to a regular latitude/longitude grid. In our results, one may note differences in the values from one climate region to another in wind and shear probability distributions, where these are generally higher in the subtropics and midlatitudes. The median and mean wind profiles are mostly overlapping, while this is not the case for the wind shear. This is mainly due to the fact that we considered the absolute values of the shear, thus mapping negative shear values to the positive side such that the probability distribution becomes skewed. Consequently, this causes a shift of the median profiles away from the mean profiles.

[20] The highest averages of wind shear values, given by the median and the mean, are found in the subtropics at 0.008 and 0.01 s^{-1}, respectively, for the radiosondes and 0.004 and 0.005 s^{-1}, respectively, for the ECMWF model. Thus, radiosondes clearly observe more wind shear than modeled by ECMWF. These high values occur mainly around the tropopause (from 9 to 15 km) near the jet stream, which is associated with high wind values exceeding 55 m s^{-1}, and in the stratosphere. High wind shear values near the surface are apparent, which point to the presence of low-level jets as seen in the raw data (not shown). But also, it may be due to the inaccuracies of the wind or/and height measurements, since the number of rejected points during the quality control is much higher at these low levels, and known tracking artifacts exist in the SPARC radiotheodolite data set, in particular for elevation angles below 17° (Vaisala Radiotheodolite RT20, Technical manual available at http://www.vaisala.com/en/products/soundingsystemsandradiosondes/soundingsystems/Pages/RT20.aspx, 2002). The presence of a large number of extreme values near the surface, which appear as outliers, has also been observed in the raw data (not shown). However, above the boundary layer, the quality of the SPARC wind measurements is improved. The midlatitude results show similarity with the subtropics, but the magnitude of the median/mean wind shear values is smaller, as seen from both radiosonde (0.006/0.008 s^{-1}) and ECMWF (0.0025/0.0035 s^{-1}). This is due to the slowing and quickening of the jet stream, respectively, as it moves northward (toward the midlatitudes) during the warm season (late spring and summer) and southward (toward the subtropics) during the cold season (autumn and winter) [*Holton*, 1992]. In the polar region, one may see relatively high median/mean

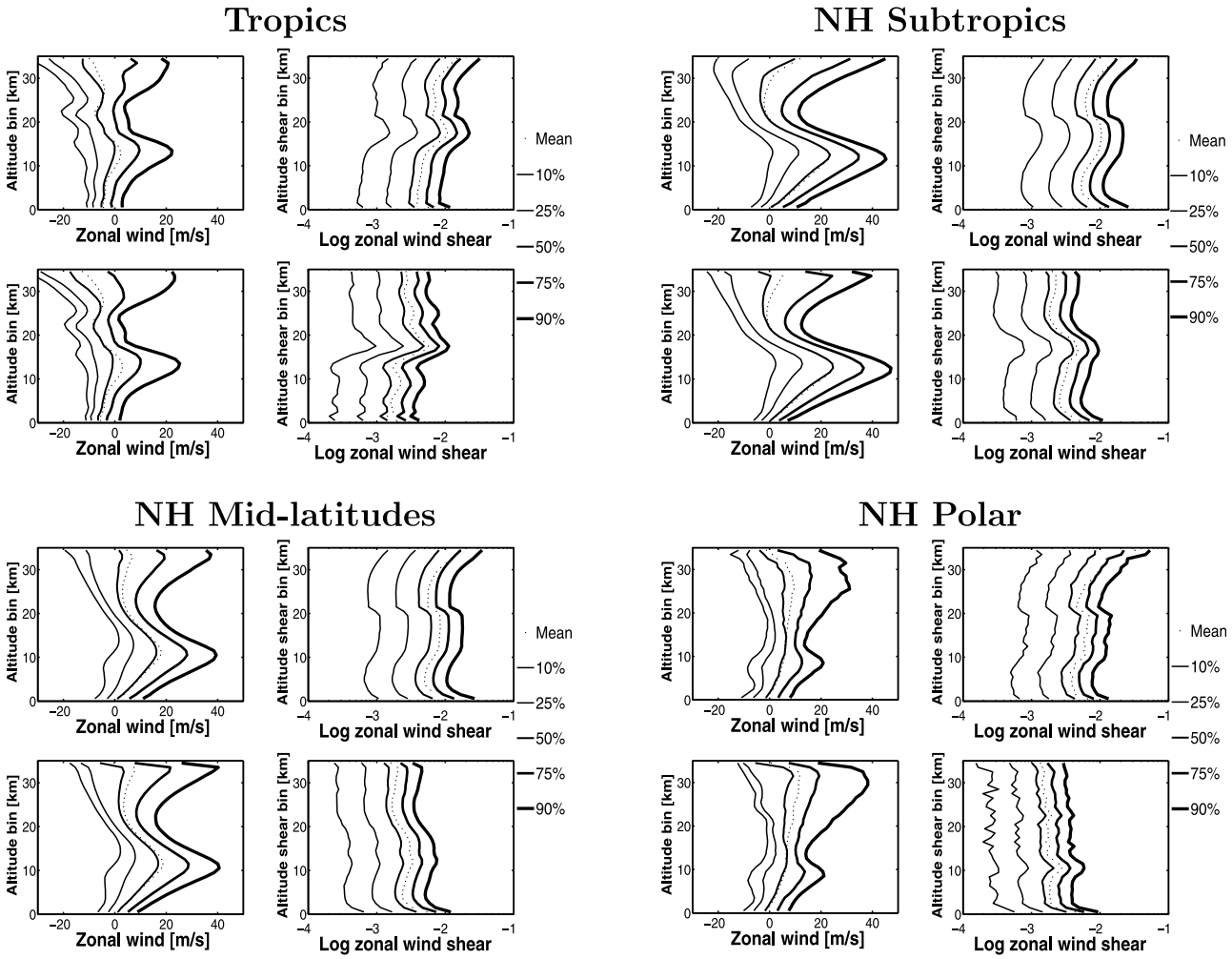

Figure 4. Zonal wind and absolute wind shear (in decadic logarithm scale) statistics for different climate regions based on high-resolution 12 s (~60 m) (top) SPARC radiosondes collocated with (bottom) ECMWF SRF: mean (dots) and percentiles (successively from left to right: 10%, 25%, 50%, 75%, and 90%); see legend at the right of each frame. The statistics are performed at each 1 km vertical bin for 1 year (2006) for both data sets. The stations are distributed over the climate zones as follows: 9 tropical, 37 subtropical, 38 midlatitudes, and 1 polar station.

values of wind shear, 0.0053/0.0065 s^{-1} from radiosonde and 0.0021/0.0030 s^{-1} from the ECMWF model, around the tropopause associated with high wind values of more than 25 m s^{-1}. In the tropics (mainly easterly wind), the highest median/mean shear values are 0.008/0.010 s^{-1} for the radiosondes against 0.005/0.006 s^{-1} for ECMWF. These maximum average values are found in the lower stratosphere, between 15 and 20 km, where the wind changes direction after a short transition around the tropopause where the wind blows westerly. Because of the lack of strong jet flows in the data, the average values of wind shear are relatively small in the polar region, as compared to the other regions. This may in turn be caused by the fact that we have only one station in the polar region. From about 25 km and up, gravity wave activity may contribute strongly to the wind and wind shear values. Some studies [*Shutts et al.*, 1988; *Kitchen and Shutts*, 1990] show that large temperature fluctuations, associated with quasi-stationary gravity waves, may lead to a strong wind shear in the horizontal wind and large variations in the balloon ascent rate. *Cadet and Teitelbaum* [1979] show that internal inertia gravity waves can accelerate the mean flow in the altitude range 20–25 km, which may explain the increase of the shear at this level and further up. Note that orographic gravity waves are parameterized in the ECMWF model and do not contribute to the statistics presented in this manuscript.

3.2.2. Meridional Wind and Wind Shear

[21] Whereas Figure 4 shows results for zonal wind, Figure 5 shows similar plots for the meridional wind and wind shear. One may notice in particular the different behavior of the two horizontal wind components, which can be seen from their variation with altitude. While the mean zonal component is generally large, the mean meridional wind tends to be around zero. This is the case, for instance, for the meridional wind in the midlatitudes and the subtropics, where the zonal wind is generally strong and dominant. The results, particularly from these two last regions where the mean/median of the meridional wind is

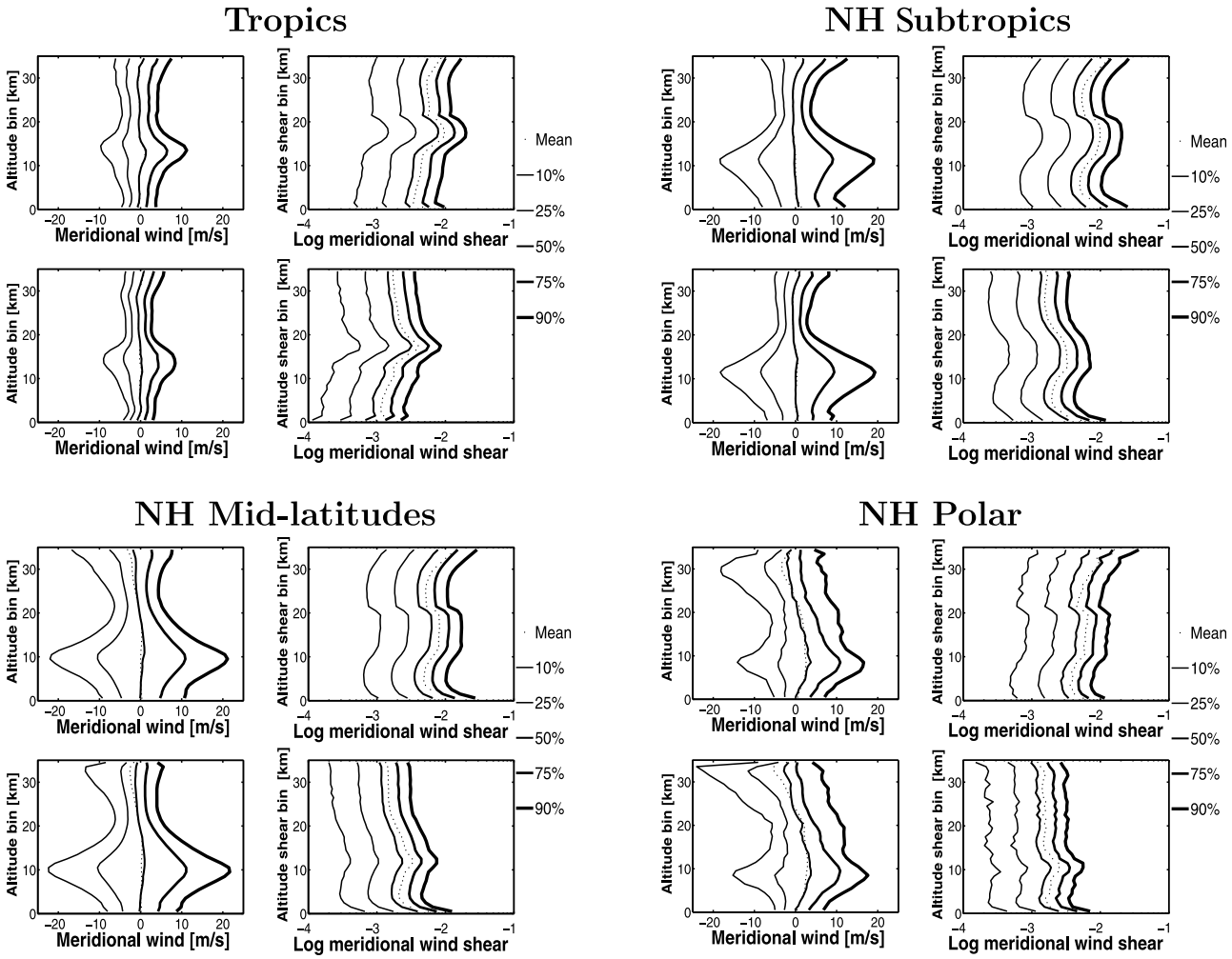

Figure 5. Same as in Figure 4, but for meridional wind. Note the different wind axis with respect to Figure 4.

close to zero at almost all levels of the atmosphere, demonstrate the different character of the zonal and meridional winds. Despite these differences, the meridional wind also produces a strong wind shear, but with magnitudes slightly smaller than the zonal wind shear. In the subtropics, for example, the mean/median values observed are 0.007/0.009 s^{-1} in the radiosondes against 0.0027/0.0035 s^{-1} for ECMWF, as opposed to the values seen in the zonal wind shear 0.008/0.010 s^{-1} for radiosondes (see also Figures 7a, 7b, and 7c of BADC and De Bilt data) and 0.004/0.005 s^{-1} for ECMWF. It is well known that zonal winds dominate the subtropics and the midlatitudes. According to these values, the ECMWF model underestimates the meridional shear by two thirds and the zonal shear by half. In the tropics, the median/mean meridional wind (mainly northerly for these Northern Hemisphere stations) increases slightly with altitude, consequently increasing the wind shear in particular around the tropopause. In the polar region, these average values of wind are increasing southerly up to the tropopause, then northerly in the stratosphere. For wind shear, substantial values are seen near the polar jet around the tropopause and in the stratosphere due to the frequent occurrence of gravity waves, as seen at this single polar station.

3.2.3. Radiosonde Drift

[22] It was mentioned previously that the collocation of the high-resolution radiosonde wind profiles with the ECMWF model is done only according to the radiosonde launch ground location (not following the trajectory of the balloon ascent). Therefore, we compute the radiosonde balloon drifts to check that these are negligible with respect to the spatial scale on which the climatological wind and shear pdfs change. The statistics obtained for the drift have been summarized by mean and median profiles, but only the mean profiles are shown in Figure 6a, as the results are comparable. The maximum drift is recorded in the subtropics where wind magnitudes are higher than in the other regions (see Figure 4). The median/mean maximum values are generally reached at the end of the ascent with values 68/71 km, while it is successively 63/66 km, 43/46 km, and 34/35 km in the midlatitudes, polar, and tropics. Except for the tropical region, the largest drifts are occurring during the tropopause crossing, near the jets (jet stream and polar jet), and then decreasing notably at higher altitudes in the subtropics and midlatitudes. In the polar

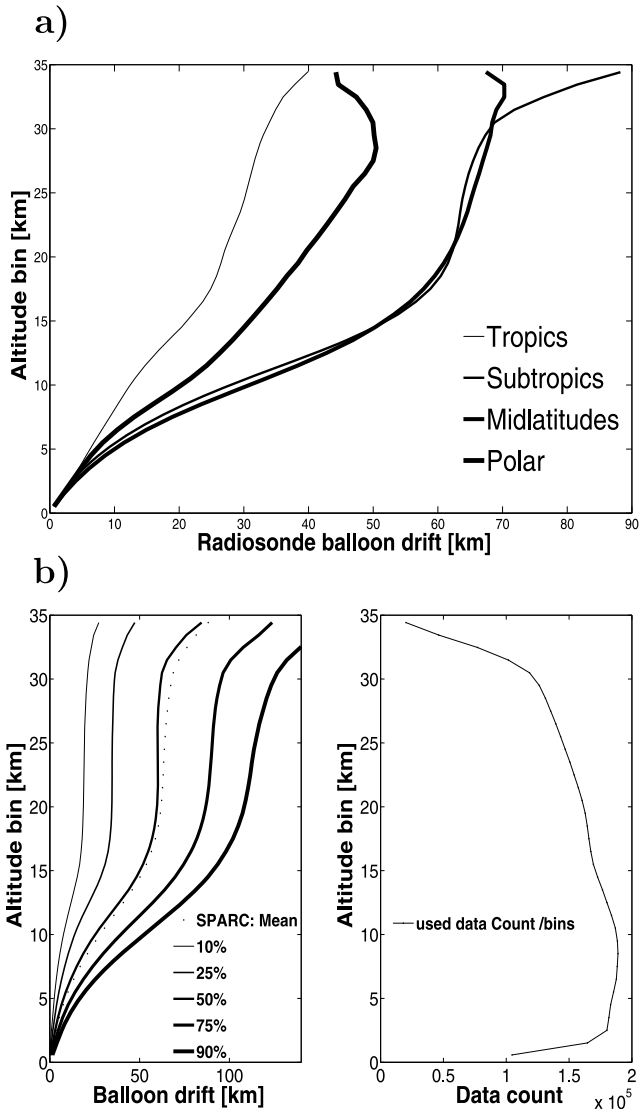

Figure 6. (a) Mean radiosonde drift over the different climate regions as shown in the legend, established from 1 year of SPARC data (2006); (b) percentile profiles as in Figure 4, but for (left) the drift and (right) the amount of data collected and used at each 1 km vertical bin, both latter in the subtropics.

region and tropics, the drift increases quasi-linearly with the ascent height. Figure 6b (left) shows percentile statistics for the radiosonde balloon drift for the maximum mean drift in the subtropics (37 stations over 2006) and where the 90% percentile reaches about 140 km in the stratosphere. From these results, we conclude that the balloon drift is usually below 100 km, which is below the ECMWF model effective horizontal resolution (~250 km). Considering these results on balloon drift, we conclude that the comparison between the radiosonde and model climates, just by applying a simple collocation according to the ground location, is valid and consistent. In addition, Figure 6b (right) shows the number of data collected at each 1 km vertical bin for the statistics in this subtropical case. This suggests that, in the first kilometer and from 30 km and up, the statistics may be not very representative of the true atmospheric dynamics because of the rejected data at these levels.

3.3. Consistency of Climate Statistics

[23] To verify how representative and consistent the statistics obtained for the 2006 SPARC data are, they are compared with similar statistics of multiyear climate established from the remaining 9 years of SPARC data for the period 1998–2007. Since the SPARC statistics are based on radiotheodolite wind-finding systems, they are also compared with other radiosonde data statistics (AMMA, BADC, and De Bilt), which are based on new generation wind-finding systems (combined LORAN and GPS). The main objective of this verification is to check on the two major issues faced in this study, as described in section 2.2, i.e., the presence of outliers in the wind observations and the limited accuracy in the shear interval (dz). These two issues are both related to the radiotheodolite wind-finding system used to collect the data.

[24] First, by following the same method as for SPARC 2006, similar statistics of the radiosonde data based on the more accurate and recent wind-finding systems, such as LORAN and GPS, are established. Figure 7 shows three examples of percentile and mean wind and shear statistics from mixed LORAN and GPS soundings for the northern (6 UK stations) and southern midlatitudes (Falkland Islands) BADC stations over the year 2006, but over 2008 for De Bilt station and collocated with the ECMWF model. The wind shear PDFs are generally similar to the northern midlatitude SPARC data, although a difference in profile shape appears due to increasing shear at the tropopause and in the low stratosphere in particular in the SPARC data. The bump in the shear at these levels in the SPARC data has been seen in the stations over and close to the extended Rocky Mountains, but also with a smaller magnitude in the stations that are far downstream. This may suggest a long-range effect of such long mountain chain. At the summit of such barriers, the flow speeds up, with monthly wind velocity of 12–15 m s^{-1} [*Barry and Chorley*, 2003] and thus high wind shear may persist. One may notice also the resemblance of statistics between the Southern Hemisphere, Northern Hemisphere, and De Bilt stations, but with remarkably higher extreme wind values in the stratosphere of the Southern Hemisphere station. Also, results from AMMA and the other BADC data sets (not shown) show similar characteristics to SPARC in the horizontal wind and shear statistics for a given climate region. Second, the remaining years of the period 1998–2007 of the SPARC data are processed, in addition to the 2006 data. Figure 8 shows the results for two selected cases, tropics and subtropics. One may see clearly that all the wind and shear profiles for the 10 years of the SPARC period resemble each other closely. Apart from the remarkable temporal variability associated with the quasi-biannual oscillation (QBO) in the tropics [*Baldwin et al.*, 2001], all values remain very similar for all profiles over this period.

3.4. Effect of the Vertical Resolution on Individual Collocated Profiles: Wind and Shear

3.4.1. Wind and Wind Shear Variability

[25] According to *Hamilton* [2006], there have been few systematic studies of the effects of vertical scaling on simulated tropospheric circulation. The goal of this subsection is to investigate the effect of reducing the vertical resolution

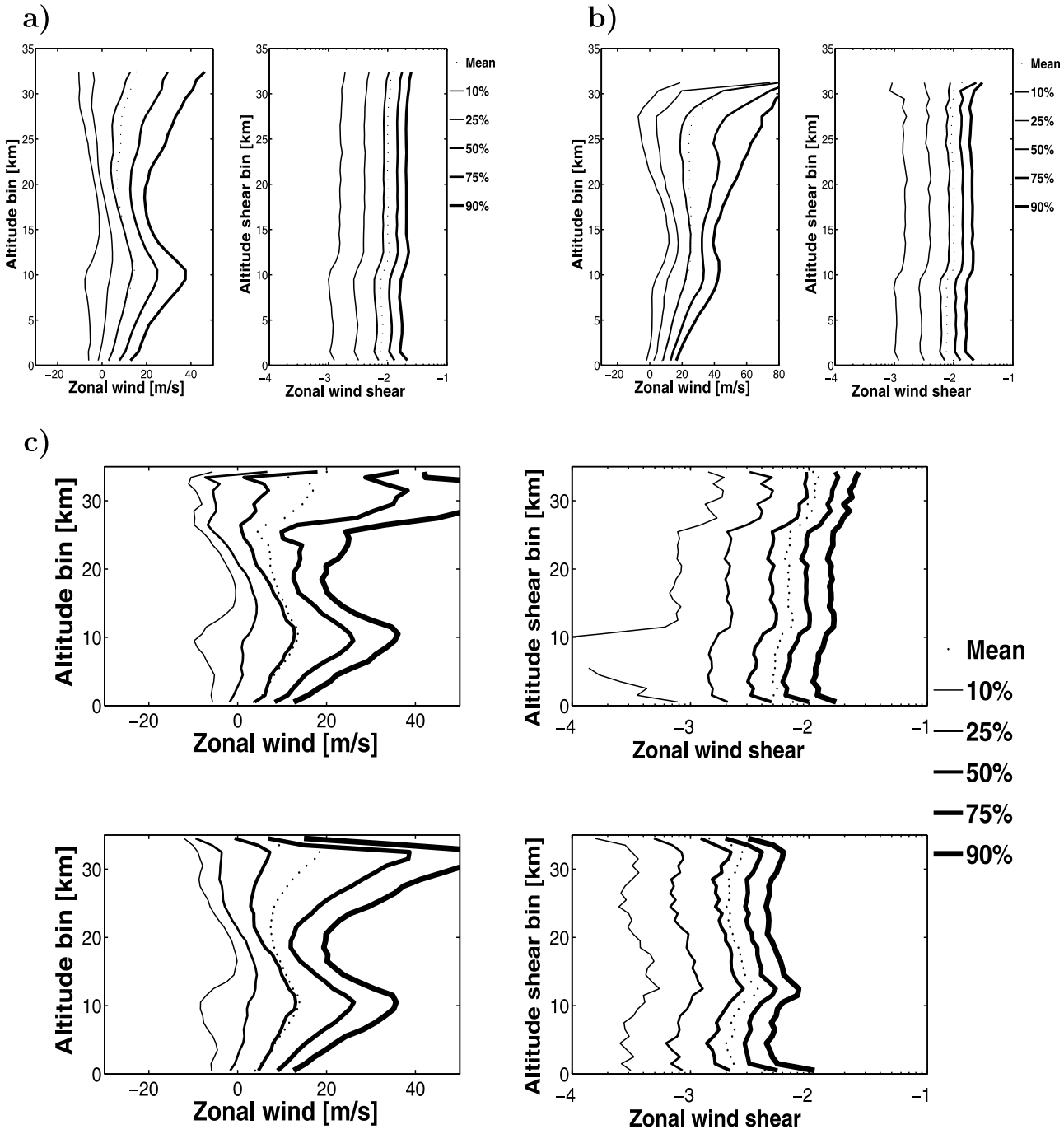

Figure 7. (a and b) Zonal wind and shear statistics at 12 s (~60 m) resolution, successively for Northern Hemisphere (6 UK stations) and Southern Hemisphere (Falkland Islands) midlatitude BADC stations over the year 2006. (c) Same as for Figures 7a and 7b, but for De Bilt station, (top) at about 50 m resolution and over the year 2008 collocated with (bottom) the ECMWF model. Notice that for De Bilt station only a few radiosoundings go higher than about 25 km; hence, the statistics are less significant. Notice also the difference of the horizontal axis for wind in Figure 7b.

on the variability of the wind and wind shear profiles of high-resolution radiosonde observations. The ECMWF profiles are taken as reference. This is achieved by applying a running mean to smooth the raw (30 m) radiosonde wind and shear profiles for successively degraded time (space) resolutions. In the wind profile analysis shown in Figure 9, the means are computed over independent time samples with lengths 6 s (raw), 24 s, 198 s (3 min 18 s), and 396 s (6 min 36 s) in order to have independent statistics. These time samples correspond approximately to vertical spatial box sizes of 30 m (raw), 120 m, 1 km, and 2 km, respectively. In addition to the mean, the standard deviation (SD) of the raw values within the box is also computed. A typical result for a subtropical station in the United States, at

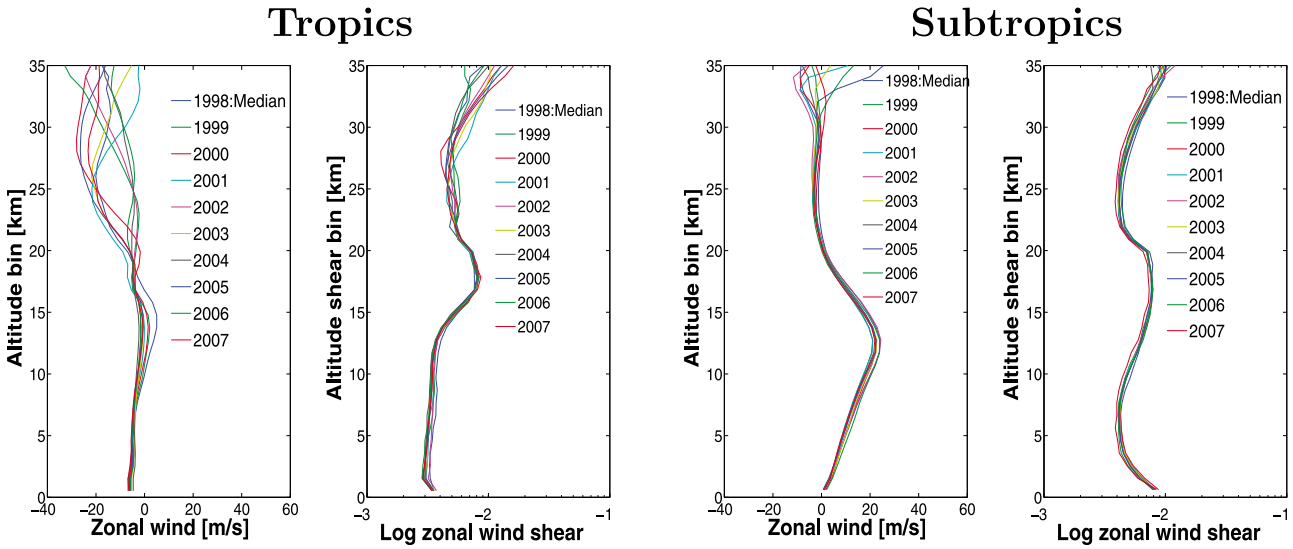

Figure 8. Interannual variability of wind and wind shear, shown by median profiles, from SPARC data for the 10 year period 1998–2007 in the (left) tropics and (right) subtropics.

90.10°W–32.3°N for the four selected box sizes is shown in Figure 9. For reference, the 12 h ECMWF forecast at its original vertical separations (see Figure 1) is given at the same ground location and time. Clearly, the lower the resolution, the better the radiosonde profile resembles the smooth ECMWF profile and the more wind variability is lost, since the SD increases. This is highlighted over the profile altitude ranges 9–14 km (Zoom 1) and 19–21 km (Zoom 2) added to Figure 9 (left). Note that the smoothness of the ECMWF profile best resembles the 2 km averaging kernel, implying a lack of wind variability in the vertical of about 2–4 m s^{-1} as indicated by the black line (SD). Occasionally, it may exceed 5 m s^{-1} near the jets and the surface and as shown here for this subtropical case at the tropopause and in the stratosphere. Compared to the ECMWF profile, the 2 km (black) profile is smoother and the 1 km (green) profile is less smooth, suggesting an effective vertical resolution of the ECMWF model, which is between 1

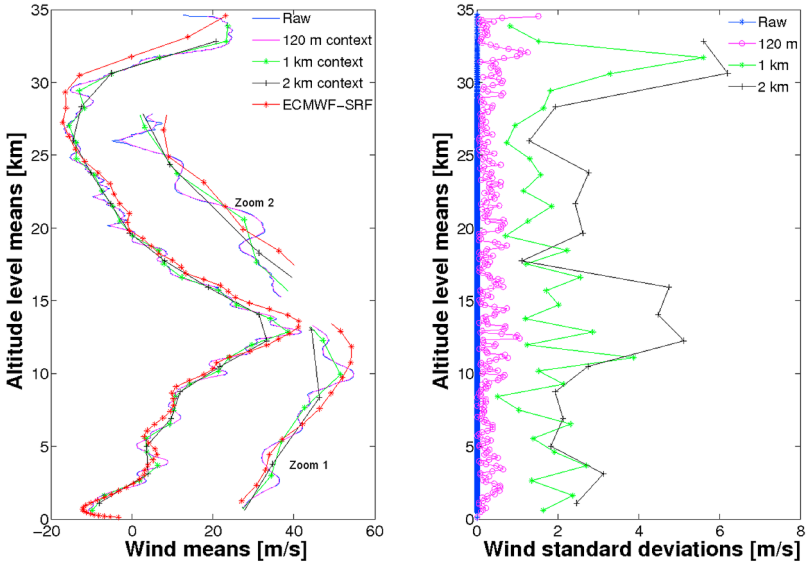

Figure 9. Effect of reducing the time (spatial) resolution of raw radiosonde zonal wind. (left) Wind profiles of radiosonde ascent for the raw 6 s (~30 m) SPARC data (blue) and for successively degraded radiosonde resolutions with moving time averages over independent samples 24 s, 198 s (3 min 18 s), and 396 s (6 min 36 s). These time samples spatially represent vertical boxes of about 120 m (magenta), 1 km (green), and 2 km (black). Notice the zooms over the altitude ranges 9–14 km (Zoom 1) and 19–21 km (Zoom 2). For comparison, the collocated ECMWF model wind profile (red) is shown on the same plot. (right) Plot showing successively, in the same colors for each box size, the standard deviation (SD) of the raw wind values in the moving box. Note that the SDs of the raw data (blue) are nullified.

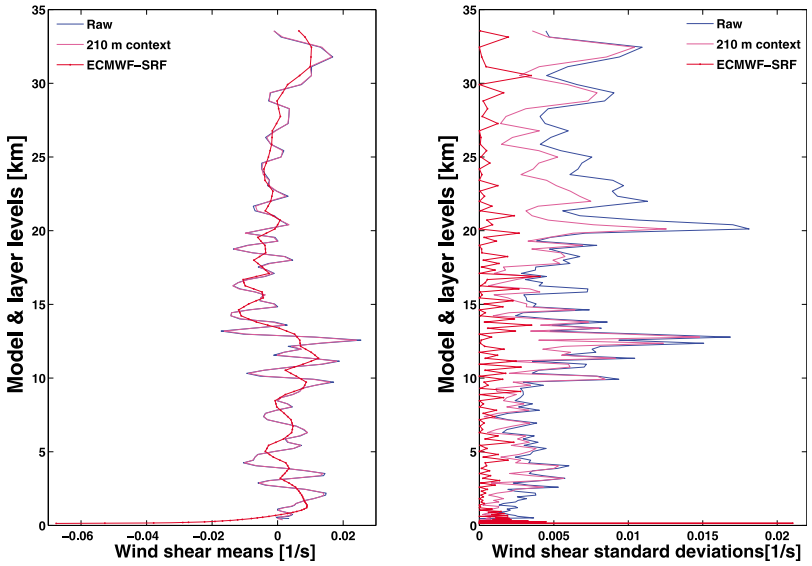

Figure 10. (left) Mean and (right) standard deviation at model and layer level altitudes of zonal wind shear profiles derived for two resolutions, 30 m (raw) and 210 m. The smoothed profile at 210 m is derived using a running mean. As a reference, the mean and standard deviation of the model wind shear profiles are also plotted. Notice that model wind shear profile is derived from an interpolated wind profile at 30 m as the raw radiosonde data.

and 2 km. One may also note that the wind profiles at 30 and 120 m contexts are very similar and the lost variability (SD) when going from 30 m to 120 m is generally small, i.e., less than 0.2 m s^{-1} for the profile in Figure 9, indicating low random measurement noise in the radiosonde. In other words, both profiles at resolutions of 30 and 120 m show similar statistics when compared to 1 and 2 km smoothed profiles, and most wind shear variance is present on scales larger than 120 m. This is in line with *Da Silveira et al.* [2001] and *Nash et al.* [2005]. *Nash et al.* [2005] estimated in particular the random errors, using the standard deviations of wind differences of various radiosondes types, to be between typically 0.2 and 0.4 m s^{-1} in the troposphere and between 0.3 and 0.5 m s^{-1} elsewhere.

[26] The effect of the vertical resolution on the shear of the zonal wind (seen in Figure 9) is more explicitly shown in Figure 10. As in the analysis of Figure 9, in Figure 10 and also in Figure 11, smooth wind profiles are first derived using running mean, but the resampling of the raw radiosonde is done for sample sizes (resolutions) of 60, 90, 120, 150, 180, 210, 330, 1000, and 2000 m. Notice that only the raw and 210 m profiles are plotted in Figure 10. In order to

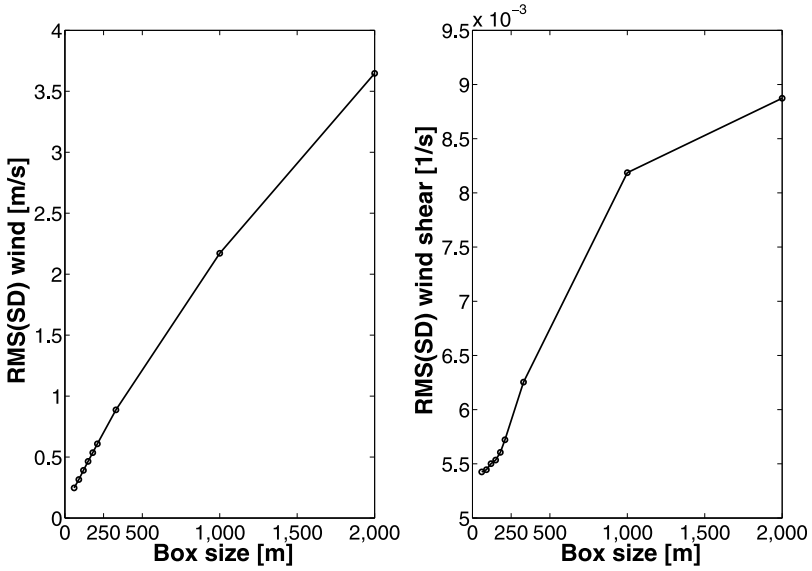

Figure 11. Square root of the mean variance of dependent samples of (left) wind and (right) wind shear in successively increased vertical box sizes, i.e., degraded resolutions, of 60, 90, 120, 150, 180, 210, 330, 1000, and 2000 m (circles), averaged over the full profile.

obtain smooth profiles, we applied the running mean using dependent samples, i.e., the shift forward between one sample to another in the profile is only by half the sample size. Wind shear profiles are computed from these smoothed wind profiles, then mean values (Figure 10, left) and standard deviations (Figure 10, right) are reported at the model levels (middle of the layers) and at intermediate levels with layer thickness from one model level to the next for a fair comparison with the model. Notice that the intermediate levels are added in order to have smooth profiles when computing the mean and SD values by overlapping wind shear values over half layers (Nyquist sampling). Notice also that the model wind shear profile is derived from interpolated wind profiles at 30 m to match the raw radiosonde data.

[27] From Figure 10 (left), we conclude that the ECMWF model vertical wind shear is smoother than the raw and smoothed 210 m radiosonde profiles. And from the left plot, considering the 210 m wind shear profile as a reference, the smoothness of the model implies a missing variability of the wind shear with values between about 0.005 and 0.01 s^{-1} on average. Differences in the wind shear variability between model and radiosonde are more pronounced at certain levels of the atmosphere, e.g., near the jets and the stratosphere, where values may exceed even 0.015 s^{-1}. We can also see that the 210 m smoothed profile closely follows the raw profile, implying a generally small loss of variability by smoothing on this scale. In the next paragraph, the change in the variability of wind and wind shear by vertical smoothing is investigated in more detail.

3.4.2. Variability and Noise

[28] Figures 9 and 10 show rather uniform statistics in the vertical. To further investigate the noise and variability properties of radiosondes and ECMWF model, we process wind and shear values in successively increased vertical box sizes, i.e., degraded resolutions, of 60, 90, 120, 150, 180, 210, 330, 1000, and 2000 m and average the obtained statistics over the full profile. We use the following definition (equation (3)),

$$\mathrm{RMS(SD)} = \sqrt{\frac{1}{\mathrm{Ns}}\sum_{j=1}^{\mathrm{Ns}}\frac{1}{\mathrm{Np}-1}\sum_{i=1}^{\mathrm{Np}}(x_i - x_m)^2}, \qquad (3)$$

while x_i are the values of the profile time series of zonal wind and wind shear, Np and x_m are successively the number of x_i values and the sample mean in each chosen resampling box of size p and Ns is the number of samples in a profile. Ns can either be independent samples or overlapping samples. For a radiosonde profile of size N (typically 1700 for the raw data), Ns = floor (N/Np) independent boxes exist; for overlapping by a factor 2 (Nyquist sampling), Ns = floor (2(N − Np)/Np).

[29] The square root of the mean variance of dependent samples of wind (left) and wind shear (right) are shown in Figure 11. Note that white instrument noise would show up as a constant level of variance (SD), but here we observe increasing variance in increasing box sizes, indicative of vertically coherent wind or shear structures. We extrapolate the RMS variance curves to a box of size one and obtain an estimate of the random error level of about 0.1 m s^{-1} and 0.005 s^{-1} for wind and shear, respectively. Given the large number of independent samples in a profile, the estimated standard error is well below 0.01 m s^{-1} and 0.0005 s^{-1} for wind and shear, respectively. Moreover, for shear, white noise dominates the variance in the radiosonde data for box sizes smaller than about 150 m. For larger box sizes, the natural shear variability dominates the shear variance

3.5. Effect of Vertical Scaling on Wind Shear Statistics: Model Effective Vertical Resolution

[30] It is shown previously that the vertical gradient of the horizontal wind (shear) is underestimated in the ECMWF model as compared to the radiosonde observations. To evaluate the degree of difference in the wind shear distributions and examine the effect of the vertical scaling on the wind shear statistics, we compare the shear statistics obtained at each 1 km vertical bin for different radiosonde vertical box sizes with the ECMWF model. This is done by computing the ratio of observation and model quantities (equation (4)). Note that the mean and median profiles of zonal and meridional wind shear were computed, but only the median ratio profiles are shown in Figure 12.

$$R_{dz}(z) = \frac{|\mathrm{Vsh}_{dz}(z)|_{\mathrm{RS}}}{|\mathrm{Vsh}(z)|_{\mathrm{EC}}}, \qquad (4)$$

where Vsh is the mean or the median of the absolute zonal (u) or meridional (v) wind shear, z denotes the center altitude of the bin and dz is the successively degraded vertical resolutions (box sizes) of the radiosonde data: 2 × 6 s (~60 m), 16 × 6 s (~480 m), 30 × 6 s (~900 m), 44 × 6 s (~1320 m), 58 × 6 s (~1740 m), and 72 × 6 s (~2160 m). Again, the spatial resolution values between brackets are given as guidance by assuming a mean ascent rate of the balloon of 5 m s^{-1}.

[31] The effect of vertical scaling on the wind shear statistics is first investigated by reducing the vertical resolution of the SPARC radiosonde data. Then, the ratios of the wind shear median/mean profiles of these radiosondes at different resolutions and ECMWF are computed following equation (4). This is done for both zonal and meridional absolute wind shear. The results in Figure 12 (only median shown) show a proportional decrease in the wind shear ratios when reducing the radiosonde vertical resolution at all different level of the atmosphere. In line with this, *Essenwanger and Reiter* [1969] demonstrated, by using a military wind rocket, the existence of a power law between the vertical wind shear and shear interval (dz), which explains the dependence of the wind shear on the spatial vertical resolution. Figure 12 also shows a decrease in the average horizontal wind shear until it reaches the amount of average shear seen in the ECMWF model (R = 1). Notice that this decrease in the average wind shear is also seen when ratios of standard deviation or ratios of interquartile shear distances are used, rather than median or mean ratios. The SPARC and ECMWF model median ratio profiles, for both zonal and meridional winds, are close to one for a radiosonde resolution 1740 m. This indicates a typical effective vertical resolution of the ECMWF model of 1.7 km, at least in the free troposphere and in particular for the meridional wind shear. In the upper stratosphere, the effective vertical resolution of the ECMWF model seems poor (>2 km) mainly because of the coarse vertical model levels, but also the imperfect subgrid scale gravity wave parameterization in this part of the atmosphere. *Koshyk et al.* [1999] showed, by

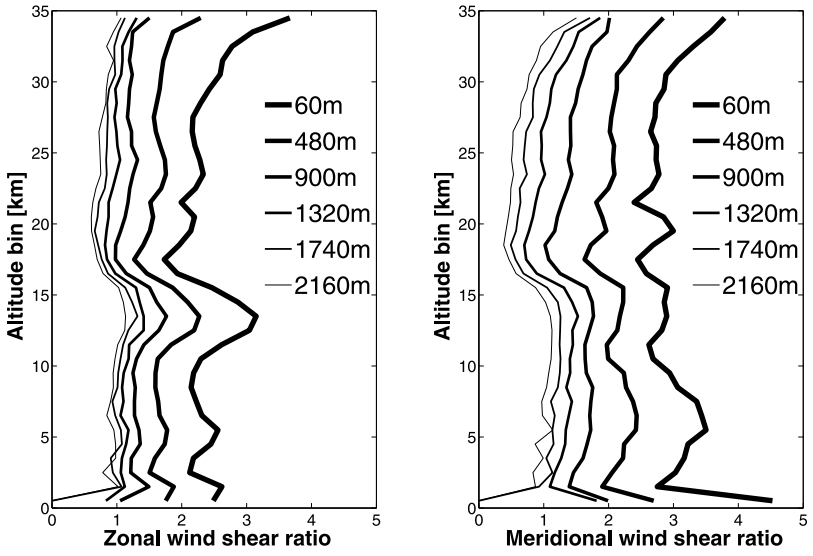

Figure 12. (left) Zonal and (right) meridional wind shear ratios of series of successively degraded radiosonde resolutions and the ECMWF model. The two plots are based on median profiles. This example is from subtropics, and similar underestimation of wind shear has been found in the other climate regions.

comparing spectra from high- and low-resolution versions of the same model, that subgrid scale parameterizations are not representing adequately the effects of the unresolved scales in middle atmosphere. The absence of nonorographic gravity waves in the ECMWF model, for example, will amplify the model wind errors.

[32] In the planetary boundary layer (PBL) where the vertical model levels of the ECMWF model are very dense, the effective vertical resolution does not appear much refined, where one may particularly notice that the wind shear ratios remain above one for the profiles with radiosonde resolution of 1.32 km. Since the model level separation is small, this draws attention to subgrid scale parameterization rather than to model level separation. *Palmer* [2001] suggests that some of the remaining errors in weather and climate prediction models may have their origin in neglecting some subgrid-scale variability in current parameterization schemes. Above the jet stream (around 17–20 km), the model effective resolution seems to be improved to about 1 km. This is due to the overestimation of the jet level wind and wind shear in the model near the jet, as can be seen from the subtropical statistics of Figures 4 and 5.

4. Conclusions

[33] In this study, we describe the atmospheric climate wind dynamics using collocated high-resolution radiosonde observations and the ECMWF model for short-range forecast (SRF). The results for the horizontal wind from both data sets are consistent, since they reproduce pretty similar averages (mean and median) and variability at different levels of the atmosphere and over the various climate regions, as defined in this study. In fact, these results are as expected, since it is seen in most collocated model radiosonde profiles, that the smooth ECMWF model wind profiles compare generally well in shape with the high-resolution profiles. However, with respect to the radiosondes, important small-scale vertical structures with high vertical wind gradients are lacking in the ECMWF profiles. Consequently, it is found that the average and climate variability of the wind shear is largely underestimated in the ECMWF model as revealed in the statistics. By comparing the statistics of successively in resolution degraded radiosonde profiles with the ECMWF model, the degree of difference in wind shear appears to be a factor of about 2.5 for the zonal wind and a factor of 3 for the meridional wind. Consequently, the effective vertical resolution of the ECMWF model is determined to be typically 1.7 km. It is moreover found that the radiosonde balloon drift is generally smaller than 100 km. Following the observation that the effective horizontal ECMWF model resolution is larger with a value of about 250 km, we conclude that the comparison between the climates of the ECMWF model and the radiosonde observations in this study is quite valid and consistent, even though the collocation of the radiosonde profiles is performed according to the radiosonde ground location. In addition, it is verified that the wind and shear climate statistics from radiotheodolite wind-finding systems (SPARC data) and from more recent wind-finding systems (LORAN and GPS) are comparable. The climate statistics obtained for 2006 from the SPARC data thus appear valid. The interannual variability computed from 10 years of SPARC data shows a large consistency of the annual climate, as well as some variability due to the QBO.

[34] This study highlights the difference in the representation of the atmospheric wind by the ECMWF model and radiosonde observations. We demonstrate in particular that on the one hand the ECMWF model is well capable of simulating the horizontal wind climate and its variability, but on the other hand it is deficient in the wind shear climate and its variability. The effect of vertical smoothing on individual collocated radiosonde model wind and wind shear profiles is investigated using four reduced resolutions. This shows mainly that the wind and wind shear variabilities that are on average lost by smoothing to the ECMWF vertical resolution appears to be 2–4 m s^{-1} for wind and 0.01–0.015 s^{-1} for wind shear, respectively, when reducing

radiosonde resolution from about 30 m to 2 km vertical resolution. But these values may exceed 5 m s^{-1} (wind) and 0.015 s^{-1} (shear) near the jets. The lack of vertical wind shear in the ECMWF model may have implications for the parameterizations of turbulence, gravity wave drag, and convection, which, ideally, should be resolution dependent.

[35] Besides the importance of this study for NWP and climate modeling, it is used as an immediate application in the framework of ESA's ADM-Aeolus to investigate the optimal vertical sampling of the Aeolus Doppler wind lidar, planned for launch in 2012. The Aeolus DWL has a limited number of vertical range bins (24) that need to be distributed in an optimal way, such that the maximum information content on wind and shear may be obtained from the atmosphere by the mission. This study is thus exploited to build a global and dynamically and optically realistic atmospheric database needed for the simulation of the Aeolus DWL, where adjustments are made to ECMWF winds to obtain a wind and shear climate compatible with the radiosonde database described in this manuscript. For more details, see *Stoffelen et al.* [2009].

[36] **Acknowledgments.** Many thanks to all the people who helped us to gather the high-resolution radiosonde data and who provided support: Stefan Liess from the SPARC project, Guillaume Brissebrat from AMMA, David Hooper and his team from BADC (UK Met-Office), and Marc Allaart, Jitze van der Meulen, Henk Klein Baltink, and Ge Verver from KNMI who made De Bilt high-resolution radiosonde data available. We also thank Dominique Lucas from ECMWF and Anton Verhoef at KNMI for their support for technical computing science issues and Davit Tan from ECMWF for his review and comments on the manuscript. This work is supported by a grant from the Dutch Ministry of Water and Transport and has been carried out in the context of the European Space Agency (ESA) contract 20940/07/NL/JA. SPARC high-resolution radiosonde data in this paper were provided by Canadian Stratospheric Processes and Their Role in Climate Network (C-SPARC) funded by Canadian Foundation for Climate and Atmospheric Sciences and the Canadian Space Agency. BADC high-resolution radiosonde data are provided courtesy of the Met Office [*UK Meteorological Office*, 2009] through the British Atmospheric Data Centre. On the basis of a French initiative, AMMA was built by an international scientific group and is currently funded by a large number of agencies, especially from France, United Kingdom, United States, and Africa. It has been the beneficiary of a major financial contribution from the European Community's Sixth Framework Research Programme. Detailed information on scientific coordination and funding is available on the AMMA International Web site http://www.amma-international.org.

References

Allen, S. J., and R. A. Vincent (1995), Gravity wave activity in the lower atmosphere: Seasonal and latitudinal variations, *J. Geophys. Res.*, *100*(D1), 1327–1350, doi:10.1029/94JD02688.

Baldwin, M. P., et al. (2001), The quasi-biennial oscillation, *Rev. Geophys.*, *39*, 179–229.

Barry, R. G., and R. J. Chorley (2003), *Atmosphere, Weather and Climate*, 8th ed., chap. 6, 421 pp., Routledge, London.

Bechtold, P., et al. (2008), Advances in simulating atmospheric variability with the ECMWF model: From synoptic to decadal time scales, *Q. J. R. Meteorol. Soc.*, *134*, 1337–1351.

Brettle, M. J., and J. F. P. Galvin (2003), Radiosondes: Part 1. The instrument, *Weather*, *57*, 336–341.

Brock, F. V., and S. J. Richardson (2001), *Meteorological Measurement System*, pp. 213–229, Oxford Univ. Press, New York.

Cadet, D., and H. Teitelbaum (1979), Observational evidence of internal inertia-gravity waves in the tropical stratosphere, *J. Atmos. Sci.*, *36*, 892–907.

Da Silveira, R., G. F. Fisc, L. A. Machado, A. M. Dall'Antonia Jr., L. F. Sapucci, D. Fernandes, R. Marques (2001), The WMO Intercomparison of GPS Radiosondes, final report, Alcantâra, Brazil.

DiMego, G. J., P. A. Phoebus, and J. E. McDonnel (1985), Data Processing and Quality Control for Optimum Interpolation Analysis at the National Meteorological Center, NMC Office Note 306, 38 pp., NOAA, U.S. Dept. of Commerce, Washington D.C.

Durre, I., R. S. Vose, and D. B. Wuertz (2006), Overview of the integrated global radiosonde archive national climatic data center, Asheville, North Carolina, *J. Clim.*, *19*, 53–68.

Essenwanger, O., and E. R. Reiter (1969), Power spectrum, structure function, vertical wind shear, and turbulence in troposphere and stratosphere, *Arch. Met. Geoph. Biokl. Ser. A*, *18*, 17–24.

Galvin, J. F. P. (2003), Radiosondes: Part 2. Using and interpreting the data, *Weather*, *58*, 387–395.

Håkansson, M. (2001), Determination of atmospheric wind statistics, *Ph. D. thesis, Dep. of Meteorol.*, Stokholm Univ., Stokholm.

Hamilton, K. (2006), High-resolution global modeling of the atmospheric circulation, *Adv. Atoms Sci.*, *23*(6), 842–856.

Hamilton, K., and R. A. Vincent (1995), High-resolution radiosonde data offer new prospects for research, *Eos Trans. AGU*, *76*(49), 497–497.

Holton, J. R. (1992), *An Introduction to Dynamic Meteorology*, 3rd ed., Academic, San Diego, Calif.

Kitchen, M., and G. J. Shutts (1990), Radiosonde observations of large-amplitude gravity waves in the lower and middle stratosphere, *J. Geophys. Res.*, *95*(D12), 20,451–20,455, doi:10.1029/JD095iD12p20451.

Koshyk, J. N., B. A. Boville, K. Hamilton, E. Manzini, and K. Shibata (1999), The kinetic energy spectrum of horizontal motions in middle atmosphere models, *J. Geophys. Res.*, *104*(D22), 27,177–27,190, doi:10.1029/1999JD900814.

Marseille, G. J., A. Stoffelen, and J. Barkmeijer (2008a), Sensitivity Observing System Experiment (SOSE): A new effective NWP-based tool in designing the global observing system, *Tellus, Ser. A*, *60*(2), 216–233.

Marseille, G. J., A. Stoffelen, and J. Barkmeijer (2008b), Impact assessment of prospective spaceborne Doppler wind lidar, *Tellus, Ser. A*, *60*(2), 234–248.

Marseille, G. J., A. Stoffelen, and J. Barkmeijer (2008c), A cycled sensitivity observing system experiment on simulated Doppler wind lidar data during the 1999 Christmas storm 'Martin', *Tellus, Ser. A*, *60*, 2,249–2,260.

Nash, J., R. Smout, T. Oakley, B. Pathack, S. Kurnosenko (2005), The WMO Intercomparison of Radiosonde Systems, final report, Vacoas, Mauritius.

National Climatic Data Center (NCDC) (1998), Data and Documentation for Rawinsonde 6-Second Data Set. (Available at ftp://atmos.sparc.sunysb.edu/pub/sparc/hres/)

Office of the Federal Coordinator for Meteorology (OFCM) (2006), Rawinsonde and Pibal Observations, Federal Meteorol. Handbook No. 3, chap. 5, U.S. Dep. of Commerce, Washington D.C.

Palmer, T. N. (2001), A nonlinear dynamical perspective on model error: A proposal for nonlocal stochastic-dynamic parameterization in weather and climate prediction models, *Q. J. R. Meteorol. Soc.*, *127*(572), 279–304.

Riddaway, R. W. (2001), Numerical methods, ECMWF document, revised by M. Hortal, chap 6., pp. 59–75.

Skamarock, W. C. (2004), Evaluating mesoscale NWP models using kinetic energy, *Mon. Weather Rev.*, *132*, 3019–3032.

Shutts, F., et al. (1994), A multiple sounding technique for the study of gravity waves, *Q. J. R. Meteorol. Soc.*, *120*(515), pp. 59–77.

Shutts, G. J., M. Kitchen, and P. H. Hoare (1988), A large amplitude gravity wave in the lower atmosphere detected by radiosonde, *Q. J. R. Meteorol. Soc.*, *114*, 579–594.

Stoffelen, A., et al. (2005), The ADM for the global wind fields measurements, *Bull. Am. Meteorol. Soc.*, *86*, 73–87.

Stoffelen, A., G. J. Marseille, F. Bouttier, D. Vasiljevic, S. De Haan, and C. Cardinali (2006), ADM-Aeolus Doppler wind lidar observing system simulation experiment, *Q. J. R. Meteorol. Soc.*, *132*, 1927–1947.

Stoffelen, A., G. J Marseille, J. De Kloe, A. Dabas, D. Huber, and O. Reitebuch (2008), Comparison of Aeolus burst and continuous mode concepts, ver. 0.8.

Stoffelen, A., H. Körnich, G. J. Marseille, K. Houchi, and J. De Kloe (2009), Assessment of Optical and Dynamical Atmospheric Heterogeneity, ver. 0.8.

Tan, D. G. H., E. Andersson, M. Fisher, and L. Isaksen (2007), Observing-system impact assessment using a data assimilation ensemble technique: Application to the ADM-Aeolus wind profiling mission, *Q. J. R. Meteorol. Soc.*, *133*, 381–390.

UK Met Office (2009), UK High-resolution Radiosonde Data, [Internet], British Atmospheric Data Centre, 2006–2009. (Available at http://badc.nerc.ac.uk/data/rad-highres/)

World Meteorological Organization (WMO) (2008), Status of the space-based global observing system, Louisiana.

Zagar, N., A. Stoffelen, J. G. Marseille, C. Accadia, and P. Schlussel (2008), Impact assessment of simulated Doppler wind lidars with a multivariate variational assimilation in the tropics, *Mon. Weather. Rev.*, *136*, 2443–2460.

J. De Kloe, K. Houchi, G. J. Marseille, and A. Stoffelen, Weather Department, Royal Netherlands Meteorological Institute, Wilhelminalaan 10, NL-3732 GK, De Bilt, Netherlands. (karim.houchi@knmi.nl)